Novel Augmented Quaternion UKF for Enhanced Loosely Coupled GPS/INS Integration

Ahmed M. Elsergany, Mamoun F. Abdel-Hafez, *Senior Member, IEEE*, and Mohammad A. Jaradat

***Abstract*— This article presents a novel direct filtering approach for loosely coupled global positioning system (GPS) and inertial navigation system (INS) integration. The proposed model is established based on utilizing the full nonlinear INS state equations in a direct configuration while including vehicle orientation through a unit-quaternion representation. A novel augmented quaternion unscented Kalman filter (AQUKF) is developed and proposed to address the direct nonlinear estimation of vehicle states for outdoor vehicle localization while preserving the non-Euclidean geometry of unit-quaternions. The proposed filter is experimentally validated under full GPS coverage as well as prolonged GPS outages. Results obtained in this article show that the proposed filter outperforms other existing solutions in various experimental testing scenarios.**

***Index Terms*— Global positioning system (GPS)/inertial navigation system (INS), Kalman filter (KF), navigation, outdoor localization, sensor fusion, unit-quaternion.**

I. Introduction

ACCURATE vehicle localization is crucial for the navigation of unmanned ground vehicles (UGVs) and unmanned aerial vehicles (UAVs) [1], [2], [3]. It is the process by which instantaneous vehicle states such as position, velocity, and attitude are estimated based on the information available from onboard sensors. Vehicles used for outdoor applications rely on outdoor localization strategies for their navigation. The global positioning system (GPS) is a commonly used sensor for accurate vehicle positioning from which other vehicle states are derived. However, despite its high accuracy, the sensor typically has a low sampling rate, and its signal is easily interrupted by structures which decreases the GPS reliability for continuous vehicle localization [4], [5]. Alternatively, an inertial measurement unit (IMU) with a high sampling frequency is used to measure a vehicle's acceleration and angular velocities which are recursively integrated in time with known initial conditions to provide a continuous estimate of vehicle states. This recursive algorithm is known as dead reckoning (DR) [6], [7] and will often lead to a diverging solution from accumulating error due to the time integral of noisy inertial sensor measurements. Together the IMU and the DR algorithm make up the inertial navigation system (INS) which is a very common approach used for vehicle localization due to its high sampling rate and continuous state estimation. However, the INS requires an aiding system with accurate localization information to periodically reset the initial conditions used by the DR algorithm to improve estimation accuracy. Therefore, a GPS/INS coupling is used to overcome the limitations of each standalone system and deliver an accurate localization solution for outdoor navigation applications.

The GPS/INS coupling requires a sensor fusion algorithm that mathematically combines their individual solutions together. The most common GPS/INS sensor fusion approach found in literature is the discrete-time Kalman filter (KF) [8]; particularly, the extended KF (EKF) variant which is extended to include the fusion of nonlinear systems [9]. The EKF uses a first-order Taylor series expansion to linearize nonlinear system equations around the current state estimate. Therefore, to use the EKF for GPS/INS fusion, researchers developed an indirect estimation strategy that linearizes the INS kinematic equations into an error model. In this approach, the difference in the INS solution and the GPS measurements is used to estimate the INS error, which is then used to correct the INS solution, hence the name indirect estimation. This form of EKF-based indirect fusion is the most reported in the literature for GPS/INS integration [10], [11], [12], [13], [14], [15], [16], [17]. However, the EKF only works well in the region where the first-order linearization sufficiently approximates the nonlinear function, which is not always the case in practice [18].

Alternatively, the unscented KF (UKF) [19], [20] was developed to overcome the EKF's need for system linearization. Instead, the UKF uses a deterministic sampling technique known as the unscented transformation (UT) through which a finite number of weighted sigma points are propagated through the nonlinear system models to provide a better approximate of the state's probability distribution rather than approximating the nonlinear function. The UKF is well studied and is proven to yield high-accuracy state estimates in many applications [21], [22], [23] including GPS/INS fusion [24], [25]. However, Zhang and Li [24] and Hu et al. [25] chose to use indirect GPS/INS integration which does not take advantage of the UKF's full potential in handling nonlinear systems. Therefore, this article intends to use a direct GPS/INS fusion algorithm based on the UKF to avoid system linearization and utilize the full nonlinear INS state model.

Manuscript received 2 April 2024; revised 25 June 2024; accepted 29 June 2024. This work was supported in part by the American University of Sharjah (AUS) Post-Doctoral Support Program and in part by the Open Access Program from American University of Sharjah. Recommended by Associate Editor M. Abbaszadeh. *(Corresponding author: Mamoun F. Abdel-Hafez.)*

Ahmed M. Elsergany and Mamoun F. Abdel-Hafez are with the Department of Mechanical Engineering, American University of Sharjah, Sharjah, United Arab Emirates (e-mail: aelsergany@aus.edu; mabdelhafez@aus.edu).

Mohammad A. Jaradat is with the Department of Mechanical Engineering, American University of Sharjah, Sharjah, United Arab Emirates, and also with the Department of Mechanical Engineering, Jordan University of Science and Technology, Irbid 22110, Jordan (e-mail: mjaradat@aus.edu).

Digital Object Identifier 10.1109/TCST.2024.3425211

The use of a direct estimation strategy for GPS/INS integration is not an entirely new concept and was first introduced in [26] using a linear state model utilizing INS acceleration as input to the filter. Another study [27] uses an EKF to directly estimate the INS states based on linearized state equations. Recently a direct UKF that uses the INS nonlinear kinematic model was proposed in [28] which delivers promising results. However, the authors represent vehicle attitude using Euler angles which are known to occasionally run into singularities that may lead to inaccurate representation of vehicle orientation. Furthermore, the Euler representation is computationally intensive due to the use of trigonometric functions in their rotation matrix parametrization [29]. Therefore, there is room for improving attitude estimation and the computational cost of direct GPS/INS integration that were not addressed in [28].

A more computationally efficient and singularity-free approach to representing vehicle attitude is the use of unit-quaternions. However, unit-quaternions do not pertain to the Euclidean vector space and do not obey traditional mathematical operations [30], [31]. This creates a challenge in using a UKF for the direct estimation of unit-quaternions due to its UT equations. Hence, if left untreated, the added uncertainty in the direct estimation of unit-quaternions using a traditional UKF will lead to a suboptimal GPS/INS state estimate. Therefore, this article proposes a novel direct GPS/INS fusion algorithm that uses nonlinear INS kinematic model augmented with unit-quaternion states named the augmented quaternion UKF (AQUKF). The proposed filter is intended to overcome the linearization and indirect estimation limitations of EKF based fusion while simultaneously addressing the concerns associated with quaternion estimation of a traditional UKF. Table I compares the proposed work to existing literature and highlights the key contributions of this article. These can be summarized as follows.

1) Develop a direct nonlinear GPS/INS fusion approach based on the UKF algorithm that overcomes the limitations of the linearized error model EKF.
2) Address the issues with Euler-based GPS/INS fusion by developing an augmented quaternion GPS/INS model for enhanced fusion accuracy based on a newly proposed AQUKF. The AQUKF is developed to take care of non-Euclidean unit-quaternions mathematics for improved attitude estimation.
3) Experimentally validate the proposed GPS/INS fusion approach under real-world trajectory with simulated GPS outages and noisy low-cost IMU.

The rest of this article is organized as follows: Section II, provides a detailed description of the GPS/INS integration in terms of system kinematic and measurement models. Section III outlines the formulation of the proposed filtering algorithm. In Section IV, the experimental setup is highlighted, and the obtained results are presented and discussed in Section V. Finally, the findings of this article are concluded in Section VI.

II. GPS/INS Integration

A GPS/INS-based integration relies on the use of GPS measurements to correct the diverging INS solution. In the proposed direct fusion approach, we model the system kinematics using INS equations augmented with quaternion states for improved estimation accuracy. Meanwhile, the measurement model is constructed using GPS output information.

A. INS Kinematic Model

The INS used in this article consists of a strapdown IMU attached to the vehicle's body. The IMU uses three mutually orthogonal accelerometers and gyroscopes for measuring vehicle's acceleration and angular velocity, respectively. All measurements are made with respect to the Earth-centered inertial (ECI) frame and resolved in the body frame. A mechanization algorithm is used to transform IMU measurements into position, velocity, and attitude information. IMU measurements are obtained as three specific body frame specific forces F^B and three body frame angular velocities ω_{IB}^B that measure the vehicle's rotation with respect to the ECI frame. The letters B and I are used to denote the body and ECI frames, respectively. IMU measured output is modeled as follows:

$$\bar{F}^B = F^B + b_a^B \tag{1}$$

$$\bar{\omega}_{IB}^B = \omega_{IB}^B + b_g^B \tag{2}$$

where $\bar{F}^{\mathrm{B}}$ and $\bar{\omega}_{IB}^B$ are the IMU bias corrupted measurements. Meanwhile, b_a^B and b_g^B are body frame accelerometer bias and gyroscope drift, respectively, modeled as a first-order Gauss-Markov process described by the following equations [32]:

$$\dot{b}_a^B = -\beta_a b_a^B + \sqrt{2\beta_a \sigma_{ag}^2} w_a \tag{3}$$

$$\dot{b}_g^B = -\beta_g b_g^B + \sqrt{2\beta_g \sigma_g^2} w_g \tag{4}$$

where β is the reciprocal of the correlation time process, w is a zero-mean uncorrelated Gaussian noise vector, and σ^2 is the variance of the white noise associated with the random process. Please note that all variables are denoted with subscripts a and g for accelerometer and gyroscope, respectively.

Since the body frame is attached to the vehicle, the INS mechanization is performed with respect to another fixed computational frame, which is chosen as the Earth-centered-Earth-fixed (ECEF) and is denoted by the letter E. Gyroscope measurements are used to define the orientation of the body frame with respect to the computational ECEF frame at any given time. Such orientation is defined by a rotation matrix that transforms any physical quantity from the body frame to the ECEF frame and is denoted by C_B^E. Therefore the following equation is used to propagate this rotation matrix in time using gyroscopic measurements:

$$\dot{C}_B^E = C_B^E \Omega_{EB}^B \tag{5}$$

where Ω_{EB}^B is the 3×3 skew-symmetric matrix of $\omega_{EB}^B = [\omega_x \ \omega_y \ \omega_z]^{\mathrm{T}}$. The latter is the angular velocity of the body frame with respect to the ECEF frame resolved in the body frame and calculated according to the following equation:

$$\omega_{EB}^B = \omega_{IB}^B - C_B^{E^{\mathrm{T}}} \omega_{IE}^E \tag{6}$$

where ω_{IB}^B is the gyroscope measurement vector and $\omega_{IE}^E = [0 \ 0 \ \omega_E]^{\mathrm{T}}$ is the Earth's angular velocity vector with respect

TABLE I
COMPARISON OF COMMON LOOSELY COUPLED GPS/INS FUSION TECHNIQUES FOUND IN LITERATURE

Study	Dynamic model	Attitude model	Kalman Filter
[11], [13-16]	Indirect/error model	Euler	EKF
[10], [12], [17]	Indirect/error model	Quaternion	EKF
[24], [25]	Indirect/error model	Euler	UKF
[26],[27]	Direct	Euler	EKF
[28]	Direct	Euler	UKF
This work	Direct	Quaternion	UKF

to the ECI frame resolved in the ECEF frame with ω_E being the Earth's rotation rate.

Equation (6) cannot be solved in a closed form and requires numerical integration which is achieved by parametrizing the rotation matrix. The three most common methods are Euler angles, direction cosine matrices (DCMs), and unit-quaternion parametrization. The unit-quaternion approach is considered the most effective way of parametrizing the rotation matrix due to its low computational cost and ability to provide singularity free solution at all possible orientations [32].

A unit-quaternion describing the rotation between the body frame and the ECEF frame $q_B^E = [q_0\ q_1\ q_2\ q_3]^{\mathrm{T}}$ is constrained to a nonlinear Riemannian manifold inside a 4-D unit sphere. Such constraint is described mathematically according to the following equation:

$$q_0^2 + q_1^2 + q_2^2 + q_3^2 = 1. \tag{7}$$

The unit-quaternion q_B^E is used to parametrize the rotation matrix C_B^E as follows:

$$C_B^E = \begin{bmatrix} q_o^2+q_1^2-q_2^2-q_3^2 & 2(q_1q_2-q_0q_3) & 2(q_1q_3+q_oq_2) \\ 2(q_1q_2+q_oq_3) & q_o^2-q_1^2+q_2^2-q_3^2 & 2(q_2q_3-q_oq_1) \\ 2(q_1q_3-q_oq_2) & 2(q_2q_3+q_oq_1) & q_o^2-q_1^2-q_2^2+q_3^2 \end{bmatrix}. \tag{8}$$

The quaternion parameters are a function of time and are propagated dynamically accordingly

$$\dot{q}_B^E = \frac{1}{2}\bar{\Omega}_{EB}^B q_B^E \tag{9}$$

where $\bar{\Omega}_{EB}^B$ is the 4×4 skew-symmetric matrix of ω_{EB}^B written in the following form:

$$\bar{\Omega}_{EB}^B = \begin{bmatrix} 0 & -\omega_{EB_x}^B & -\omega_{EB_y}^B & -\omega_{EB_z}^B \\ \omega_{EB_x}^B & 0 & \omega_{EB_Z}^B & -\omega_{EB_y}^B \\ \omega_{EB_y}^B & -\omega_{EB_Z}^B & 0 & \omega_{EB_x}^B \\ \omega_{EB_Z}^B & \omega_{EB_y}^B & -\omega_{EB_x}^B & 0 \end{bmatrix}. \tag{10}$$

In this article, we use (9) instead of (5) to represent vehicle orientation at all times to simplify and improve the GPS/INS integration.

The vehicle's measured specific force is integrated to obtain the vehicle's translational states which consist of its position and velocity. The vehicle's acceleration is derived in the ECEF frame as follows [10]:

$$\dot{V}^E = C_B^E F^B - 2\Omega_{IE}^E V^E - {\Omega_{IE}^E}^2 P^E + G^E \tag{11}$$

where Ω_{IE}^E is the 3×3 skew-symmetric matrix of ω_{IE}^E and G^E is the gravitational vector in the E-frame [10].

The vehicle's velocity V^E is obtained by integrating (11) which is integrated further to obtain the vehicle's position P^E represented as follows:

$$\dot{P}^E = V^E. \tag{12}$$

The full INS state vector, (13) consists of the orientation between the body frame and the ECEF frame described by a unit-quaternion, the vehicle's position, and velocity in the ECEF frame, and the sensors bias. Therefore, the nonlinear state equations are summarized by the following equation (14):

$$x_t = \begin{bmatrix} q_B^E & V^E & P^E & b_a^B & b_g^B \end{bmatrix}^{\mathrm{T}} \tag{13}$$

$$\begin{bmatrix} \dot{q}_B^E \\ \dot{V}^E \\ \dot{P}^E \\ \dot{b}_a^B \\ \dot{b}_g^B \end{bmatrix} = \begin{bmatrix} \frac{1}{2}\bar{\Omega}_{EB}^B q_B^E \\ C_B^E F^B - 2\Omega_{IE}^E V^E - {\Omega_{IE}^E}^2 P^E + G^E \\ V^E \\ -\beta_a b_a^B \\ -\beta_g b_g^B \end{bmatrix} + \begin{bmatrix} 0_{4x1} \\ 0_{3x1} \\ 0_{3x1} \\ \sqrt{2\beta\sigma_{ba}^2} \\ \sqrt{2\beta\sigma_{bg}^2} \end{bmatrix} w. \tag{14}$$

Equation (14) is a continuous time process model described as follows:

$$\dot{x}_t = \Phi(x_t) + \Gamma w_t \tag{15}$$

where x_t and w_t are continuous-time state vectors and process noise, respectively. $\Phi(.)$ is a nonlinear continuous-time state-transition function and Γ is process noise distribution vector. However, to use a KF-based GPS/INS fusion algorithm a discretization step is necessary, using sensor sampling time ΔT to get the system in the following equation:

$$x_{k+1} = f(x_k) + \Gamma \Delta T w_k \tag{16}$$

where x_k and w_k are discrete-time state vector and process noise, respectively, observed at discrete-time step k. $f(.)$ in this case is a discrete-time nonlinear function derived from $\Phi(.)$ of (14) using improved Euler discretization [33].

In contrast to other existing GPS/INS models [11], [13], [14], [15], [16], [34], [35], the proposed approach augments the vehicle's attitude as unit-quaternion within the INS equations, allowing for its direct estimation at a lower computational cost alongside position, velocity, and sensor bias states for improved estimation accuracy.

B. Measurement Model

The GPS position and velocity measurements in the ECEF frame are used for KF-based fusion. The following equation below describes the discrete-time measurement vector z_k used in this article:

$$z_k = \begin{bmatrix} V^E_{\text{Gps}} \\ P^E_{\text{GPS}} \end{bmatrix}. \tag{17}$$

By considering the state and measurement vectors of (13) and (17), respectively, a discrete-time measurement model is constructed as follows:

$$z_k = H_k x_k + v_k \tag{18}$$

where $H_k = [0_{6\times4}, I_{6\times6}, 0_{6\times6}]$ is a constant linear observation matrix and $v_k \in \mathbb{R}^m$ is uncorrelated zero-mean Gaussian white measurement noise with covariance matrix $E[v_k v_k^{\mathrm{T}}] = R_k$.

III. Proposed Filter Formulation

In this article, a UKF is chosen for the purpose of improving GPS/INS fusion accuracy by avoiding system linearization. However, many studies [36], [37] show that a traditional UKF is not suitable for the nonlinear estimation of unit-quaternion states that are augmented in the proposed novel direct nonlinear INS model of (14). This is due to the fact that UKF does not consider the non-Euclidean geometry of a constrained unit-quaternion. Therefore, we propose a parallel fusion scheme that incorporates a quaternion-based UKF to simultaneously satisfy the unit-quaternion geometry constraint while staying relevant to the nonquaternion states and measurements involved in the proposed GPS/INS direct fusion model presented earlier.

The unit-quaternion mathematical operations are to be introduced initially before the formulation of the proposed AQUKF filtering model.

A. Unit-Quaternion Operations

Unit-quaternions have a unique set of mathematical relations and operations due to them being constrained to a 4-D Riemannian manifold. Therefore, it is important to establish the mathematics necessary to constraint the equations of a traditional UKF for the nonlinear filtering of unit-quaternions.

Given $q_a = (v_a, n_a)$ and $q_b = (v_b, n_b)$ as two different unit-quaternions where v and n are real and imaginary components, respectively, their product is described as follows [30]:

$$q_a \otimes q_b = \left[v_a v_b - n_a^{\mathrm{T}} n_b,\, v_a n_b + v_b n_a + n_a \times n_b\right] \tag{19}$$

where $\times$ denotes the cross-product operator.

Meanwhile, quaternion subtraction is defined as their conjugate multiplication

$$q_a \ominus q_b = q_a \otimes q_b^{-1} \tag{20}$$

where $q^{-1} = (v, -n)$.

A unit-quaternion q defines a rotation θ along an axis e of unit norm used to express the quaternion's real and imaginary components as follows:

$$q = \left[\cos\left(\frac{\theta}{2}\right), \sin\left(\frac{\theta}{2}\right)e\right]. \tag{21}$$

Following the definition in (19) a mapping between a unit-quaternion in a 4-D Riemannian manifold and a rotation vector in the 3-D Euclidean tangent space can be established. A mapping from a rotational vector r to a unit-quaternion is defined as follows:

$$q = \begin{cases} \left(\cos\left(\dfrac{\|r\|}{2}\right), \sin\left(\dfrac{\|r\|}{2}\right)\dfrac{r}{\|r\|}\right), & \text{if } \|r\| \neq 0 \\ (1, [0]_{3\times1}), & \text{if } \|r\| = 0. \end{cases} \tag{22}$$

Equation (22) is denoted by $r2q(.)$ operator for brevity. Such mapping is quite essential as it will be used as the basis for modifying UKF based equations to account for direct quaternion estimation. It is important to note that (19)–(22) will serve as the basis for developing the proposed AQUKF in Section III-B.

B. Augmented Quaternion UKF

The proposed nonlinear augmented quaternion INS state vector presented by (13) offers the flexibility of partitioning the states in to $x_1 = q_B^E$ and $x_2 = [V^E \;\; P^E \;\; b_a^B \;\; b_g^B]^{\mathrm{T}}$ representing the constrained and unconstrained states, respectively. Therefore, a partitioned continuous-time process model is proposed as follows:

$$\dot{q}_B^E = \frac{1}{2}\bar{\Omega}_{EB}^B q_B^E \tag{23}$$

$$\begin{bmatrix} \dot{V}^E \\ \dot{P}^E \\ \dot{b}_a^B \\ \dot{b}_g^B \end{bmatrix} = \begin{bmatrix} C_B^E F^B - 2\Omega_{IE}^E V^E - {\Omega_{IE}^E}^2 P^E + G^E \\ V^E \\ -\beta_a b_a^B \\ -\beta_g b_g^B \end{bmatrix}. \tag{24}$$

Equations (23) and (24) are converted into their discrete-time equivalent as presented earlier to be used by the proposed AQUKF algorithm

$$\begin{cases} x_{1_{k+1}} = f_1(x_{1_k}) + \Gamma_1 \Delta T w_{1_k} \\ x_{2_{k+1}} = f_2(x_{2_k}) + \Gamma_2 \Delta T w_{2_k} \end{cases} \tag{25}$$

where $x_{1_k} \in \mathbb{R}^l$ and $x_{2_k} \in \mathbb{R}^n$ are the constrained and unconstrained state vectors, respectively, at discrete-time step k; $w_{1_k} \in \mathbb{R}^l$ and $w_{2_k} \in \mathbb{R}^n$ are uncorrelated zero-mean Gaussian white process noise with covariance matrices $E[w_{1_k} w_{1_k}^{\mathrm{T}}] = Q_{1_k}$ and $E[w_{2_k} w_{2_k}^{\mathrm{T}}] = Q_{2_k}$; $f_{1,2}(.)$ is the discrete-time nonlinear process model.

Similar to a traditional UKF, the proposed AQUKF algorithm uses the UT approach to carefully select a set of deterministic sigma points based on the a priori mean and covariance of the given state under the Gaussian random variable (GRV) assumption. Computed sigma points are directly propagated through the nonlinear system model to provide a more accurate estimate of the state's posteriori mean and covariance.

However, since constrained and unconstrained states are involved in the filtering process, the partitioned models of (23)–(25) are used to create a parallel algorithm that allows for the simultaneous independent UT of constrained and unconstrained states followed by a parallel prediction and finally an augmented correction. The proposed model not only guarantees the accurate estimation of constrained

states by conserving their norm unity but also cuts down on computational time by running a parallel UT and prediction scheme.

The AQUKF framework involves the recursion of the following steps.

Step 1: Given a posteriori state and state covariance estimates, $\hat{x}_{k|k} = \begin{bmatrix} \hat{x}_{1_{k|k}} \\ \hat{x}_{2_{k|k}} \end{bmatrix}$ and $\hat{P}_{k|k} = \begin{bmatrix} \hat{P}_{1_{k|k}} & 0 \\ 0 & \hat{P}_{2_{k|k}} \end{bmatrix}$, respectively, obtained from the previous estimation step, a parallel sigma point transformation is performed using quaternion UT (QUT) and traditional UT, defined by (26) and (27), respectively. QUT is formulated using constrained quaternion operations introduced earlier in (19)–(22) as follows:

$$\begin{cases} \chi_{1_{i,k|k}} = \hat{x}_{1_{k|k}}, & i = 0 \\ \chi_{1_{i,k|k}} = \hat{x}_{1_{k|k}} \otimes r2q\left(\sqrt{(l+\lambda)\hat{P}_{1_{k|k}}}\right)_i, & i = 1, \ldots, l \\ \chi_{1_{i,k|k}} = \hat{x}_{1_{k|k}} \otimes r2q\left(\sqrt{(l+\lambda)\hat{P}_{1_{k|k}}}\right)_{i-l}^{-1}, & i = l+1, \ldots, 2\,l \end{cases} \tag{26}$$

where $\hat{x}_{1_{k|k}} \in \mathbb{R}^l$ and $\chi_{1_{k|k}} \in \mathbb{R}^{2l+1}$ are the a priori unit-quaternion state vector and sigma points, respectively, while $\hat{P}_{1_{k|k}}$ is the a priori state covariance associated with the unit-quaternion state vector. Furthermore, λ is a scaling parameter usually chosen in the range $[0, 1]$ while $(((l+\lambda)\hat{P}_{1_{k|k}})^{1/2})_i$ is the ith column of the matrix $((l+\lambda)\hat{P}_{1_{k|k}})^{1/2}$ computed using lower triangular Cholesky decomposition and is taken as a rotational vector. Hence, the $r2q()$ mapping is used to convert this state into a unit-quaternion where simple quaternion addition and subtraction are represented by quaternion product [38]. It is important to note that having unit-quaternion sigma points is highly important for the accurate estimation of unit-quaternion states and the overall filter's stability.

Meanwhile, the UT of nonquaternion states is performed as follows:

$$\begin{cases} \chi_{2_{i,k|k}} = \hat{x}_{2_{k|k}}, & i = 0 \\ \chi_{2_{i,k|k}} = \hat{x}_{2_{k|k}} + \left(\sqrt{(n+\kappa)\hat{P}_{2_{k|k}}}\right)_i, & i = 1, \ldots, n \\ \chi_{2_{i,k|k}} = \hat{x}_{2_{k|k}} - \left(\sqrt{(n+\kappa)\hat{P}_{2_{k|k}}}\right)_i, & i = n+1, \ldots, 2\,n \end{cases} \tag{27}$$

where $\hat{x}_{2_{k|k}} \in \mathbb{R}^n$ and $\chi_{2_k} \in \mathbb{R}^{2n+1}$ are the nonquaternion state vector and sigma points, respectively, while $\hat{P}_{2_{k|k}}$ is the state covariance associated with the nonquaternion state vector. Furthermore, κ is a scaling parameter usually chosen in the range $[0, 1]$ while $(((n+\kappa)\hat{P}_{2_{k|k}})^{1/2})_i$ is the ith column of the matrix $((n+\kappa)\hat{P}_{2_{k|k}})^{1/2}$ computed using lower triangular Cholesky decomposition.

Step 2: A priori state estimates $\hat{x}_{k+1|k}$ and state covariances $\hat{P}_{k+1|k}$ are predicted by propagating the sigma points of (26) and (27) as follows:

$$\chi_{1_{i,k+1|k}} = f_1\left(\chi_{1_{i,k|k}}\right), \quad i = 0, 1, \ldots, 2l \tag{28}$$

$$\hat{x}_{1_{k+1|k}} = \frac{\sum_{i=0}^{2l} W_i^1 \chi_{1_{i,k+1|k}}}{\left|\sum_{i=0}^{2l} W_i^1 \chi_{1_{i,k+1|k}}\right|} \tag{29}$$

where $\begin{cases} W_i^1 = (\lambda/(l+\lambda)), & i = 0 \\ W_i^1 = (\lambda/(2(l+\lambda))), & i = 1, \ldots, 2l \end{cases}$

$$\hat{P}_{1_{k+1|k}} = \sum_{i=0}^{2l} W_i^1 \left(\chi_{1_{i,k+1|k}} \ominus \hat{x}_{1_{k+1|k}}\right)\left(\chi_{1_{i,k+1|k}} \ominus \hat{x}_{1_{k+1|k}}\right)^{\mathrm{T}} + Q_1 \tag{30}$$

$$\chi_{2_{i,k+1|k}} = f_2\left(\chi_{2_{i,k|k}}\right), \quad i = 0, 1, \ldots, 2n \tag{31}$$

$$\hat{x}_{2_{k+1|k}} = \sum_{i=0}^{2n} W_i^2 \chi_{2_{i,k|k}} \tag{32}$$

where $\begin{cases} W_i^2 = (\lambda/(n+\lambda)), & i = 0 \\ W_i^2 = (\lambda/(2(n+\lambda))), & i = 1, \ldots, 2n \end{cases}$

$$\hat{P}_{2_{k+1|k}} = \sum_{i=0}^{2n} W_i^2 \left(\chi_{2_{i,k+1|k}} - \hat{x}_{2_{k+1|k}}\right)\left(\chi_{2_{i,k+1|k}} - \hat{x}_{2_{k+1|k}}\right)^{\mathrm{T}} + Q_2. \tag{33}$$

It is important to note that (28)–(30) are referred to as the constrained prediction defined exclusively for constrained unit-quaternion states. Meanwhile, (31)–(33) are the unconstrained prediction equations used for regular nonquaternion states. Accordingly, a priori state estimate $\hat{x}_{k+1|k}$ and state covariance $\hat{P}_{k+1|k}$ are augmented as indicated by (34) and (35) which are then used for the last step of the proposed algorithm AQUKF known as the augmented correction

$$\hat{x}_{k+1|k} = \begin{bmatrix} \hat{x}_{1_{k+1|k}} \\ \hat{x}_{2_{k+1|k}} \end{bmatrix} \tag{34}$$

$$\hat{P}_{k+1|k} = \begin{bmatrix} \hat{P}_{1_{k+1|k}} & 0 \\ 0 & \hat{P}_{2_{k+1|k}} \end{bmatrix}. \tag{35}$$

Step 3: A posteriori state estimate $\hat{x}_{k+1|k+1}$ and state covariance $\hat{P}_{k+1|k+1}$ are updated in an augmented correction step using newly obtained GPS measurements according to the discretized measurement model of (18).

Since the measurement model of (18) is linear and the measurements are unconstrained, the basic KF equations are used for this step to reduce the computational cost without any tradeoff in accuracy as shown in the following equations:

$$\hat{z}_{k+1|k} = H_k \hat{x}_{k+1|k} \tag{36}$$

$$S_{k+1} = H_k \hat{P}_{k+1|k} H_k^{\mathrm{T}} + R_k \tag{37}$$

$$T_{k+1} = \hat{P}_{k+1|k} H_k^{\mathrm{T}} \tag{38}$$

$$K_{k+1} = T_{k+1} S_{k+1}^{-1} \tag{39}$$

$$\hat{x}_{k+1|k+1} = \hat{x}_{k+1|k} + K_{k+1}\left(z_k - \hat{z}_{k+1|k}\right) \tag{40}$$

$$\hat{P}_{k+1|k+1} = \hat{P}_{k+1|k} - K_{k+1} S_{k+1}^{-1} K_{k+1}^{\mathrm{T}} \tag{41}$$

where S and T are the innovation covariance and cross covariance, respectively, and K is the Kalman gain.

A summary of the proposed AQUKF algorithm is illustrated in Fig. 1.

IV. Experimental Validation

The proposed algorithm is validated experimentally using low-cost strapdown IMU and GPS units mounted onto a passenger vehicle as shown in Fig. 2. The sensors used for this experimental work are a part of the Xsens MTi-G-710 series

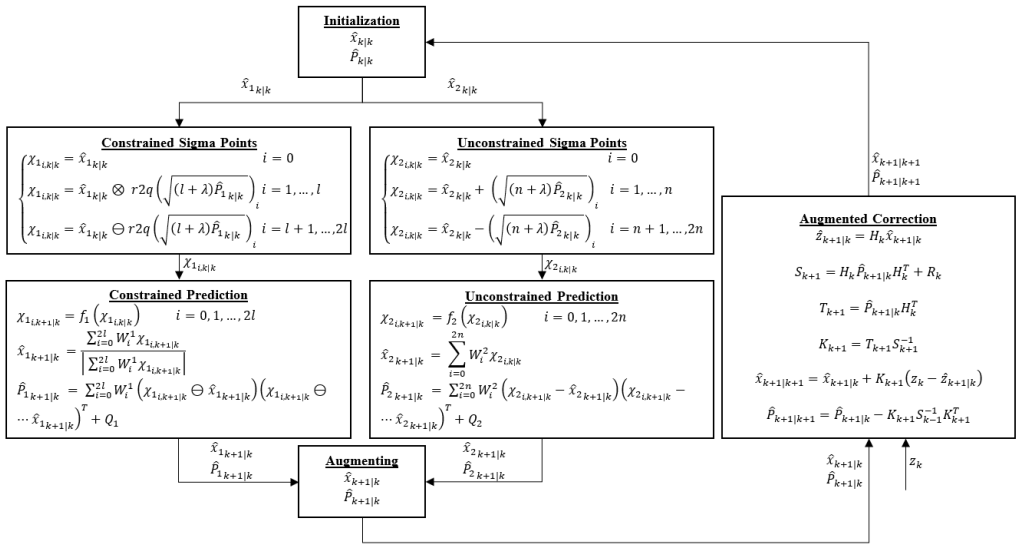

Fig. 1. Proposed AQUKF algorithm.

(a) (b)

Fig. 2. Experimental setup. (a) IMU. (b) GPS receiver.

TABLE II

IMU SPECIFICATIONS [39]

Parameter	*Accelerometer*		*Gyroscope*	
	Value	Unit	Value	Unit
Standard Full Range	200	[m/s²]	450	[°/s]
Initial Bias Error	0.05	[m/s²]	0.2	[°/s]
In-run Bias Stability	15	[μg]	10	[°/h]
Bandwidth (-3dB)	375	[Hz]	415	[Hz]
Noise Density	60	[μg/√HZ]	0.01	[°/s/√HZ]

TABLE III

GPS RECEIVER SPECIFICATIONS [39]

Parameter	Value	Unit
Update Rate	4	[Hz]
Position Accuracy	2.5	[m]
Velocity Accuracy	0.05	[m/s]
Heading	0.3	[°]
Start-up Time Cold Start	26	[s]

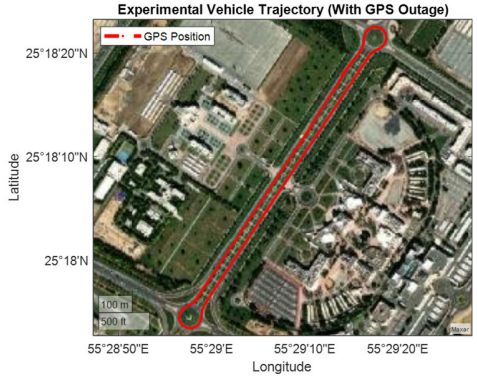

Fig. 3. Experimental vehicle trajectory without GPS outage.

manufactured by Movella and their technical specifications are summarized in Tables II and III. The IMU and GPS sensors are sampled at 400 and 4 Hz, respectively, which shows the significant difference in sampling frequency between the sensors. Therefore, this article intends to study the impact of the sampling ratio between the two sensors on fusion accuracy. To do so, a predefined trajectory is generated by driving a passenger vehicle around Sharjah University City to validate the proposed algorithm's performance under different driving conditions and maneuvers. Fig. 3 shows the GPS data of the chosen trajectory.

In addition, a GPS outage with varying lengths is simulated on the collected data at the 100 s mark of the field experiment to test the proposed solution's performance in the absence of GPS signal as illustrated on Fig. 4. This experimental environment, with the simulated GPS outages, will ensure an extensive evaluation of the performance and robustness of the proposed sensor fusion algorithm under real-world scenarios and practical conditions.

V. RESULTS AND DISCUSSION

The estimation accuracy of the proposed GPS/INS fusion algorithm is evaluated against the solution provided by the Xsens MTi-G-710 unit taken as the benchmark for this article due to its maturity. Similarly, the performance of the most

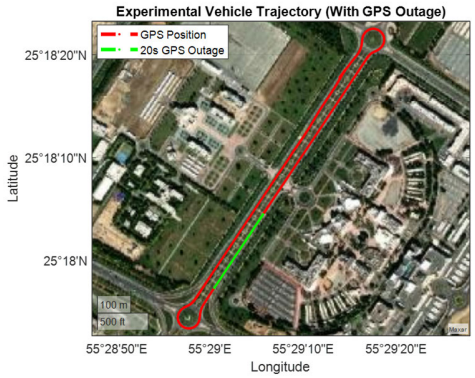

Fig. 4. Experimental vehicle trajectory with simulated GPS outage of 20 s duration.

TABLE IV
STATISTICAL ANALYSIS OF POSITION ESTIMATION ERROR

	P_x		P_y		P_z	
	Mean $[m]$	STD $[m]$	Mean $[m]$	STD $[m]$	Mean $[m]$	STD $[m]$
EKF	2.15	0.83	1.05	0.73	1.99	1.04
UKF	0.68	0.97	0.55	0.73	0.16	0.65
AQUKF	0.11	0.35	0.05	0.22	0.08	0.46
UKF[28]	0.41	0.99	0.19	0.33	0.12	0.58

TABLE V
STATISTICAL ANALYSIS OF VELOCITY ESTIMATION ERROR

	V_x		V_y		V_z	
	Mean $[m/s]$	STD $[m/s]$	Mean $[m/s]$	STD $[m/s]$	Mean $[m/s]$	STD $[m/s]$
EKF	1.89	0.94	0.90	0.76	1.76	1.05
UKF	0.30	0.24	0.83	1.17	0.37	0.61
AQUKF	0.06	0.09	0.01	0.07	0.01	0.09
UKF[28]	0.12	0.18	0.21	0.33	0.14	0.42

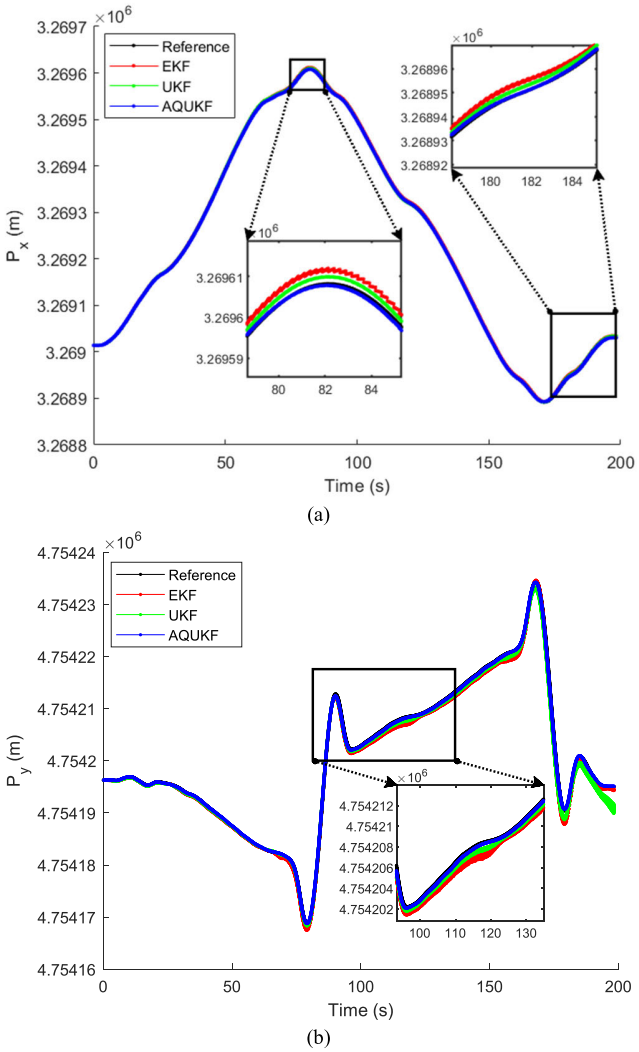

Fig. 5. ECEF position estimate versus time. (a) x-direction and (b) y-direction (without GPS outage).

cited indirect EKF [10], [11], [12], [13], [14], [15], [16], [17] as well as a traditional UKF based on the proposed direct INS are evaluated using the same reference. Qualitative and quantitative analysis of vehicle state estimates are used to carefully compare the performance of the three algorithms to study the improvements made to the GPS/INS fusion accuracy by the proposed AQUKF algorithm.

Figs. 5 and 6 provide a graphical illustration of the estimation accuracy in position and velocity, respectively, along the ECEF x- and y-directions without simulated GPS outage. Furthermore, Tables IV and V support the graphical findings of Figs. 5 and 6 by providing a statistical analysis in terms of the mean and standard deviation (STD) of the estimation errors in position and velocity, along the three orthogonal ECEF axes.

In addition, graphical representations of the attitude errors in pitch, roll, and yaw estimates representing vehicle's orientation with respect to the East North Up (ENU) navigation frame are demonstrated in Fig. 7. The mean and STD corresponding to the estimation errors of Fig. 7 are summarized in Table VI. The angular rate measurements of the low-cost gyroscope used in this article are plotted on Fig. 8 to indicate the level of noise and uncertainty handled in the fusion process. By initial inspection of the obtained results without simulated GPS outage, we can draw a conclusion that indirect EKF and traditional UKF are no contenders to the proposed AQUKF which outperforms them in the estimation of all vehicle states as demonstrated graphically by Figs. 5–7 and statistically supported by Tables IV–VI. The AQUKF is shown to maintain mean and STD values that are within satisfactory practical accuracy. An extended study is performed to measure the level of improvement in estimation accuracy provided by the UKF and AQUKF using the indirect EKF as the baseline due to being the worst performing filter out of the three. The findings of this extended study are summarized graphically in Figs. 9 and 10 to provide a visual demonstration of the improvements obtained in the error mean and STD, respectively, of the position, velocity, and attitude estimates. A negative percentage indicates a drop in performance in comparison to the EKF algorithm.

The estimation performance of the direct Euler UKF [28] is highlighted in Tables IV–VI as well as Figs. 11 and 12 without simulated GPS outages. It is found that although the Euler direct UKF has a better estimation performance than the traditional indirect EKF and UKF, it still underperforms in comparison to the proposed AQUKF. Furthermore, the average computational time of the traditional indirect EKF, UKF, direct Euler UKF [28], and the proposed AQUKF are found to be

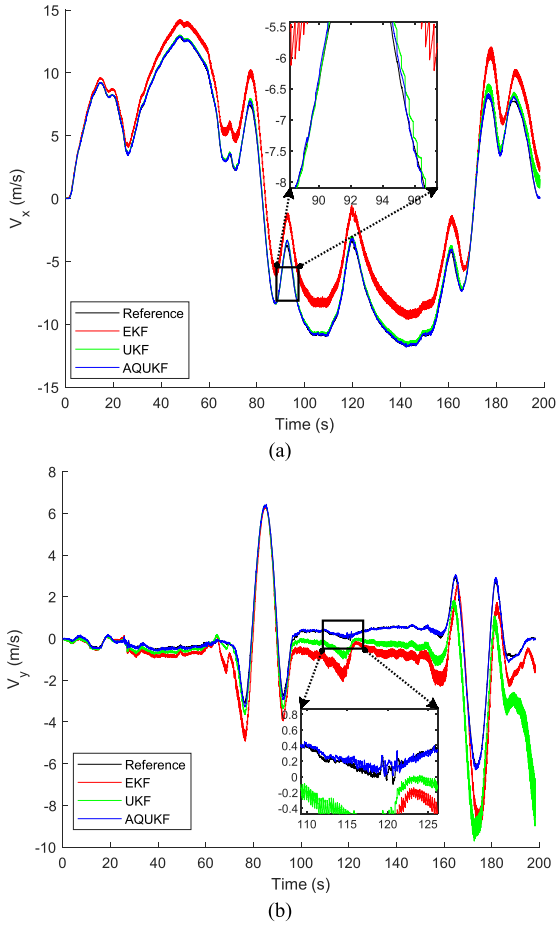

Fig. 6. ECEF velocity estimate versus time (a) x-direction and (b) y-direction (without GPS outage).

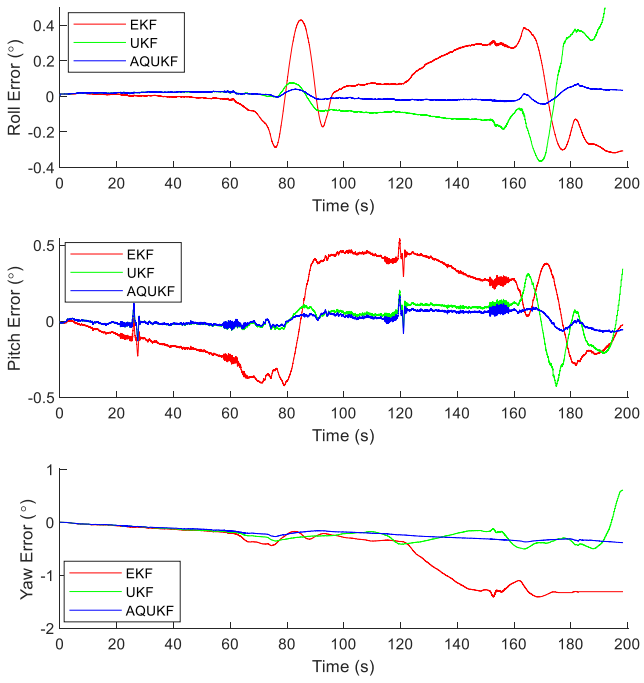

Fig. 7. Body frame to ENU attitude estimate errors versus time (without GPS outage).

1.72, 1.89, 2.52, and 2.34 ms, respectively, per iteration. It is important to note that for this real-time consideration, the

TABLE VI
STATISTICAL ANALYSIS OF ATTITUDE ESTIMATION ERROR

	Roll		*Pitch*		*Yaw*	
	Mean [°]	**STD [°]**	**Mean [°]**	**STD [°]**	**Mean [°]**	**STD [°]**
EKF	0.04	0.94	0.06	0.76	0.27	1.64
UKF	0.01	0.24	0.02	1.17	0.20	1.20
AQUKF	0.01	0.09	0.01	0.07	0.18	0.30
UKF[28]	0.01	0.07	0.01	0.15	0.19	0.82

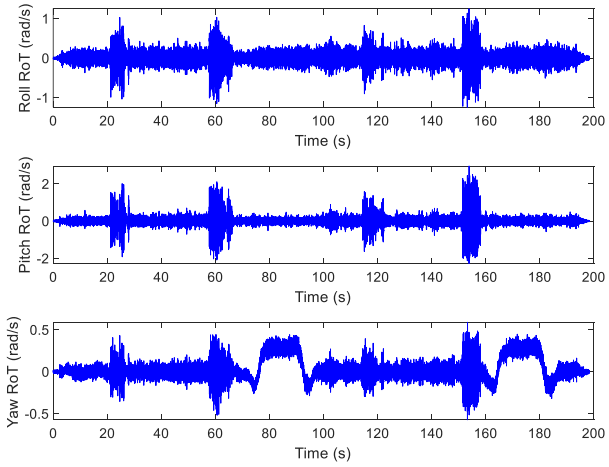

Fig. 8. Gyroscope angular rate of turn (RoT) measurements versus time.

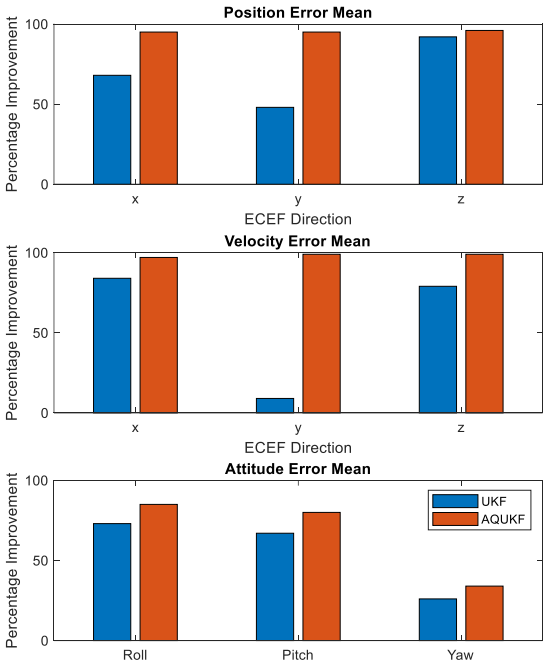

Fig. 9. Percentage improvement in error mean with respect to the EKF.

computational time per iteration has to fall below the sampling time of the IMU which is 2.50 ms for this work. Therefore, the direct Euler UKF is not practically fit for real-time estimation using a high sampling IMU.

The position estimation accuracy in the ECEF x- and y-directions during GPS outage with varying length is presented graphically in Figs. 13 and 14, respectively. In addition, Fig. 15 illustrates the statistical mean absolute error (MAE) associated with the estimation errors of Figs. 13 and 14.

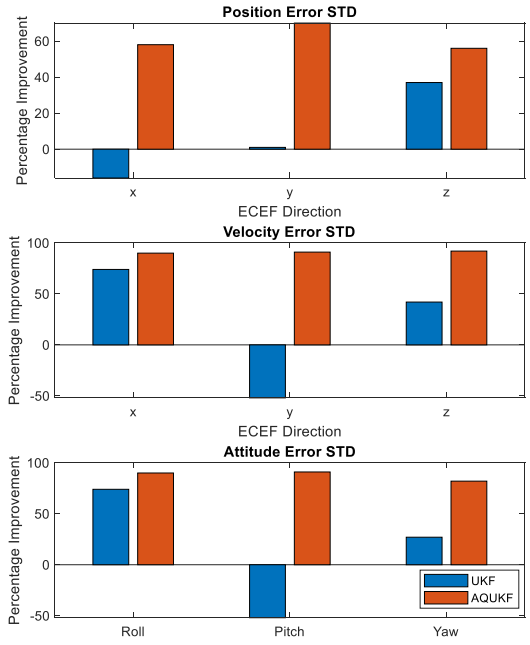

Fig. 10. Percentage improvement in error variance with respect to the EKF.

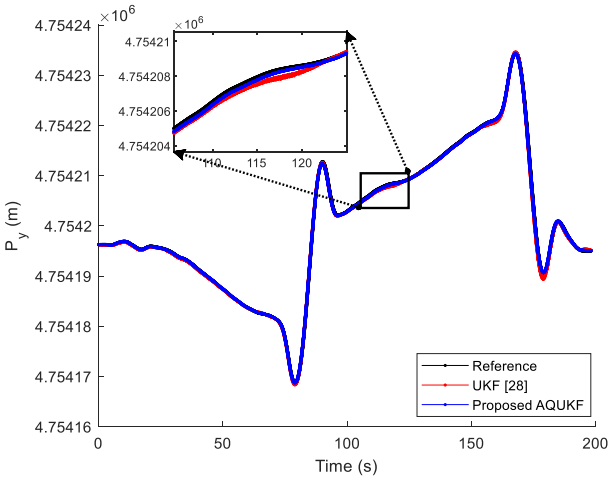

Fig. 11. ECEF position estimate comparison (without GPS outage).

Once more, the obtained results show that the AQUKF is capable of significantly minimizing INS errors in contrast to the indirect EKF and traditional UKF during GPS outages. This effect is more significant as the outage period increases indicating the importance of high accuracy estimates between successive GPS measurements used to correct IMU sensor bias and minimize INS divergence.

The presented results align with the proposed theoretical premise that direct filtering approaches that utilize the full nonlinear dynamics of GPS/INS fusion are superior to ones that rely on model linearization. This can be strictly observed in the poor performance of an indirect EKF in contrast to direct traditional UKF and the proposed direct AQUKF model. In addition, this article was presented on the basis that the accuracy of vehicle attitude information is vital for high accuracy vehicle localization. This statement is supported by the discrepancy in estimation accuracy observed between the traditional UKF and the proposed AQUKF given that

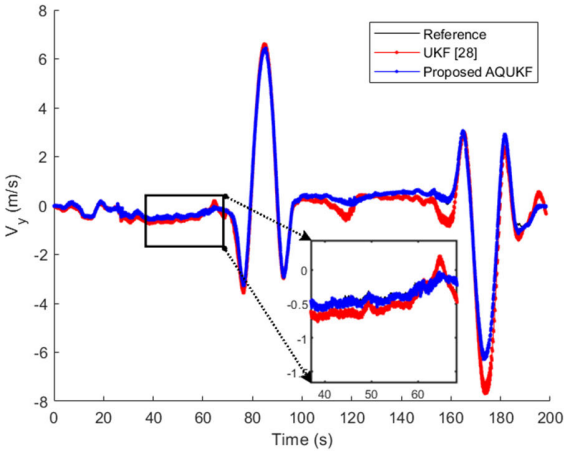

Fig. 12. ECEF velocity estimate comparison (without GPS outage).

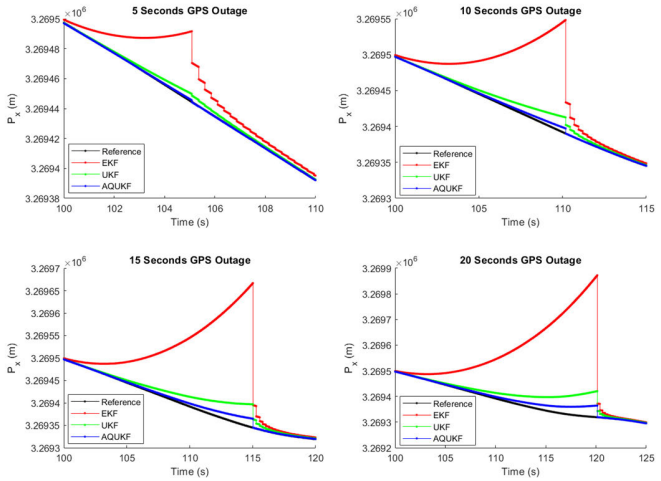

Fig. 13. ECEF x-position estimate during GPS outage of varying duration.

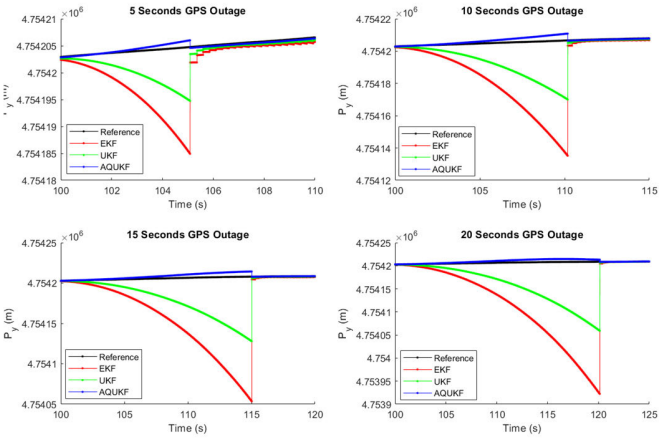

Fig. 14. ECEF y-position estimate during GPS outage of varying duration.

both use the same model with the only difference being how quaternions are propagated within the UKF equations. The results show that a direct traditional UKF can perform worse than the EKF in some cases due to the increased uncertainty in quaternion propagation as indicated by Fig. 15, further highlighting the contribution of the proposed AQUKF algorithm.

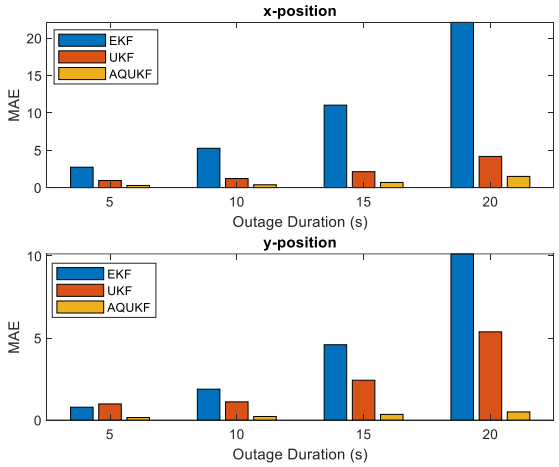

Fig. 15. MAE values in position estimates during GPS outage with varying duration.

All the obtained results indicate that the proposed AQUKF algorithm provides a high-level estimation accuracy for outdoor vehicle localization using low-cost loosely coupled GPS/INS that holds true during prolonged GPS outages.

VI. Conclusion

This article proposes a new direct filtering approach for low-cost loosely coupled GPS/INS. The contribution of this article is that a direct INS kinematic model is established which augments vehicle orientation through a unit-quaternion format. In addition, a UKF is used to utilize the full nonlinearity of the proposed direct model which is further modified to account for quaternion non-Euclidean mathematics through a novel AQUKF algorithm.

The proposed AQUKF is validated experimentally for outdoor vehicle localization of a passenger vehicle mounted with low-cost strapdown IMU and GPS sensors. The difference in sampling frequencies between the two sensors and a simulated GPS outage with varying lengths were used to evaluate the performance of the proposed solution and compare it to that of an indirect EKF and a direct traditional UKF. The obtained results support that the proposed AQUKF outperforms other alternative fusion models in all given scenarios, implying the importance of direct fusion models and uncertainty-free quaternion propagation for accurate GPS/INS fusion. It is worth noting that the proposed AQUKF is developed based on the assumption that the GPS/INS measurements are Gaussian with known covariance which is not always true in practice. Therefore, to further improve the results of this work, it is recommended to use an adaptive variant of the proposed AQUKF to handle Gaussian noise with time-variant covariance and/or non-Gaussian noise, which will be the scope of our future work. Furthermore, future research may include expanding the findings of this work to the detection of noncooperative targets with unknown positions utilizing more than two sensors.

Acknowledgment

This article represents the opinions of the author(s) and does not mean to represent the position or opinions of American University of Sharjah. The authors acknowledge the efforts of engineer Nidal A. Sherif for resourcing the data used for this article.

References

[1] Y. He, J. Li, and J. Liu, "Research on GNSS INS & GNSS/INS integrated navigation method for autonomous vehicles: A survey," *IEEE Access*, vol. 11, pp. 79033–79055, 2023, doi: 10.1109/ACCESS.2023.3299290.

[2] J. Fayyad, M. A. Jaradat, D. Gruyer, and H. Najjaran, "Deep learning sensor fusion for autonomous vehicle perception and localization: A review," *Sensors*, vol. 20, no. 15, pp. 1–34, 2020, doi: 10.3390/s20154220.

[3] P. K. Panigrahi and S. K. Bisoy, "Localization strategies for autonomous mobile robots: A review," *J. King Saud Univ.-Comput. Inf. Sci.*, vol. 34, no. 8, pp. 6019–6039, Sep. 2022, doi: 10.1016/j.jksuci.2021.02.015.

[4] M. A. K. Jaradat and M. F. Abdel-Hafez, "Enhanced, delay dependent, intelligent fusion for INS/GPS navigation system," *IEEE Sensors J.*, vol. 14, no. 5, pp. 1545–1554, May 2014, doi: 10.1109/JSEN.2014.2298896.

[5] H. Bai and R. W. Beard, "Relative heading estimation and its application in target handoff in GPS-denied environments," *IEEE Trans. Control Syst. Technol.*, vol. 27, no. 1, pp. 74–85, Jan. 2019, doi: 10.1109/TCST.2017.2773027.

[6] E. I. Al Khatib, M. A. Jaradat, M. Abdel-Hafez, and M. Roigari, "Multiple sensor fusion for mobile robot localization and navigation using the extended Kalman filter," in *Proc. 10th Int. Symp. Mechatronics Appl. (ISMA)*, Dec. 2015, pp. 1–5, doi: 10.1109/ISMA.2015.7373480.

[7] E. I. Al Khatib, M. A. K. Jaradat, and M. F. Abdel-Hafez, "Low-cost reduced navigation system for mobile robot in Indoor/Outdoor environments," *IEEE Access*, vol. 8, pp. 25014–25026, 2020, doi: 10.1109/ACCESS.2020.2971169.

[8] R. E. Kalman, "A new approach to linear filtering and prediction problems," *J. Basic Eng.*, vol. 82, no. 1, pp. 35–45, Mar. 1960.

[9] M. I. Ribeiro, "Kalman and extended Kalman filters: Concept, derivatison and properties," Inst. Syst. Robot., Portugal, Tech. Rep. 62, 2004.

[10] M. F. Abdel-Hafez, "The autocovariance least-squares technique for GPS measurement noise estimation," *IEEE Trans. Veh. Technol.*, vol. 59, no. 2, pp. 574–588, Feb. 2010, doi: 10.1109/TVT.2009.2034969.

[11] Y. Zhang, "A fusion methodology to bridge GPS outages for INS/GPS integrated navigation system," *IEEE Access*, vol. 7, pp. 61296–61306, 2019, doi: 10.1109/ACCESS.2019.2911025.

[12] M. F. Abdel-Hafez, K. Saadeddin, and M. A. Jarrah, "Constrained low-cost GPS/INS filter with encoder bias estimation for ground vehicles' applications," *Mech. Syst. Signal Process.*, vols. 58–59, pp. 285–297, Jun. 2015, doi: 10.1016/j.ymssp.2014.12.012.

[13] Y. Liu, Q. Luo, and Y. Zhou, "Deep learning-enabled fusion to bridge GPS outages for INS/GPS integrated navigation," *IEEE Sensors J.*, vol. 22, no. 9, pp. 8974–8985, May 2022, doi: 10.1109/JSEN.2022.3155166.

[14] E. S. Abdolkarimi, M. R. Mosavi, S. Rafatnia, and D. Martín, "A hybrid data fusion approach to AI-assisted indirect centralized integrated SINS/GNSS navigation system during GNSS outage," *IEEE Access*, vol. 9, pp. 100827–100838, 2021, doi: 10.1109/ACCESS.2021.3096422.

[15] Y. Yao, X. Xu, C. Zhu, and C.-Y. Chan, "A hybrid fusion algorithm for GPS/INS integration during GPS outages," *Measurement*, vol. 103, pp. 42–51, Jun. 2017, doi: 10.1016/j.measurement.2017.01.053.

[16] J. Liu and G. Guo, "Vehicle localization during GPS outages with extended Kalman filter and deep learning," *IEEE Trans. Instrum. Meas.*, vol. 70, pp. 1–10, 2021, doi: 10.1109/TIM.2021.3097401.

[17] W. M. F. Al-Masri, M. F. Abdel-Hafez, and M. A. Jaradat, "Inertial navigation system of pipeline inspection gauge," *IEEE Trans. Control Syst. Technol.*, vol. 28, no. 2, pp. 609–616, Mar. 2020, doi: 10.1109/TCST.2018.2879628.

[18] J. Chang, J. Cieslak, J. Dávila, J. Zhou, A. Zolghadri, and Z. Guo, "A two-step approach for an enhanced quadrotor attitude estimation via IMU data," *IEEE Trans. Control Syst. Technol.*, vol. 26, no. 3, pp. 1140–1148, May 2018, doi: 10.1109/TCST.2017.2695164.

[19] S. Julier, J. Uhlmann, and H. F. Durrant-Whyte, "A new method for the nonlinear transformation of means and covariances in filters and estimators," *IEEE Trans. Autom. Control*, vol. 45, no. 3, pp. 477–482, Mar. 2000, doi: 10.1109/9.847726.

[20] E. A. Wan and R. Van Der Merwe, "The unscented Kalman filter for nonlinear estimation," in *Proc. IEEE Adapt. Syst. Signal Process., Commun., Control Symp.* Piscataway, NJ, USA: Institute of Electrical and Electronics Engineers, Oct. 2000, pp. 153–158, doi: 10.1109/ASSPCC.2000.882463.

[21] M. Partovibakhsh and G. Liu, "An adaptive unscented Kalman filtering approach for online estimation of model parameters and state-of-charge of lithium-ion batteries for autonomous mobile robots," *IEEE Trans. Control Syst. Technol.*, vol. 23, no. 1, pp. 357–363, Jan. 2015, doi: 10.1109/TCST.2014.2317781.

[22] M. S. El Din, A. A. Hussein, and M. F. Abdel-Hafez, "Improved battery SOC estimation accuracy using a modified UKF with an adaptive cell model under real EV operating conditions," *IEEE Trans. Transport. Electrific.*, vol. 4, no. 2, pp. 408–417, Jun. 2018, doi: 10.1109/TTE.2018.2802043.

[23] A. K. Singh and B. C. Pal, "Decentralized dynamic state estimation in power systems using unscented transformation," *IEEE Trans. Power Syst.*, vol. 29, no. 2, pp. 794–804, Mar. 2014, doi: 10.1109/TPWRS.2013.2281323.

[24] Q. Zhang and B. Li, "A low-cost GPS/INS integration based on UKF and BP neural network," in *Proc. 5th Int. Conf. Intell. Control Inf. Process.*, Aug. 2014, pp. 100–107, doi: 10.1109/ICICIP.2014.7010322.

[25] G. Hu, S. Gao, and Y. Zhong, "A derivative UKF for tightly coupled INS/GPS integrated navigation," *ISA Trans.*, vol. 56, pp. 135–144, May 2015, doi: 10.1016/j.isatra.2014.10.006.

[26] H. Qi and J. B. Moore, "Direct Kalman filtering approach for GPS/INS integration," *IEEE Trans. Aerosp. Electron. Syst.*, vol. 38, no. 2, pp. 687–693, Apr. 2002, doi: 10.1109/TAES.2002.1008998.

[27] R. Munguía, "A GPS-aided inertial navigation system in direct configuration," *J. Appl. Res. Technol.*, vol. 12, no. 4, pp. 803–814, Aug. 2014, doi: 10.1016/S1665-6423(14)70096-3.

[28] G. Hu, W. Wang, Y. Zhong, B. Gao, and C. Gu, "A new direct filtering approach to INS/GNSS integration," *Aerosp. Sci. Technol.*, vol. 77, pp. 755–764, Jun. 2018, doi: 10.1016/j.ast.2018.03.040.

[29] Z.-Q. Zhang, X.-L. Meng, and J.-K. Wu, "Quaternion-based Kalman filter with vector selection for accurate orientation tracking," *IEEE Trans. Instrum. Meas.*, vol. 61, no. 10, pp. 2817–2824, Oct. 2012, doi: 10.1109/TIM.2012.2196397.

[30] A. C. B. Chiella, B. O. S. Teixeira, and G. A. S. Pereira, "Quaternion-based robust attitude estimation using an adaptive unscented Kalman filter," *Sensors*, vol. 19, no. 10, p. 2372, May 2019, doi: 10.3390/s19102372.

[31] B. J. Sipos, "Application of the manifold-constrained unscented Kalman filter," in *Proc. IEEE/ION Position, Location Navigat. Symp.*, May 2008, pp. 30–43, doi: 10.1109/PLANS.2008.4569967.

[32] A. Noureldin, T. B. Karamat, and J. Georgy, "Inertial navigation system modeling," in *Fundamentals of Inertial Navigation, Satellite-Based Positioning and Their Integration*. Berlin, Germany: Springer, 2013, pp. 167–200, doi: 10.1007/978-3-642-30466-8_5.

[33] K. Xiong, L. D. Liu, and H. Y. Zhang, "Modified unscented Kalman filtering and its application in autonomous satellite navigation," *Aerosp. Sci. Technol.*, vol. 13, nos. 4–5, pp. 238–246, Jun. 2009, doi: 10.1016/j.ast.2009.04.001.

[34] M. Aslinezhad, A. Malekijavan, and P. Abbasi, "ANN-assisted robust GPS/INS information fusion to bridge GPS outage," *EURASIP J. Wireless Commun. Netw.*, vol. 2020, no. 1, p. 129, Dec. 2020, doi: 10.1186/s13638-020-01747-9.

[35] X. Wei et al., "A mixed optimization method based on adaptive Kalman filter and wavelet neural network for INS/GPS during GPS outages," *IEEE Access*, vol. 9, pp. 47875–47886, 2021, doi: 10.1109/ACCESS.2021.3068744.

[36] K. Li, L. Chang, and Y. Chen, "Common frame based unscented quaternion estimator for inertial-integrated navigation," *IEEE/ASME Trans. Mechatronics*, vol. 23, no. 5, pp. 2413–2423, Oct. 2018, doi: 10.1109/TMECH.2018.2865757.

[37] K. Li, X. Lu, and W. Li, "Nonlinear error model based on quaternion for the INS: Analysis and comparison," *IEEE Trans. Veh. Technol.*, vol. 70, no. 1, pp. 263–272, Jan. 2021, doi: 10.1109/TVT.2020.3046680.

[38] J. Sola. (2015). *Quaternion Kinematics for the Error-State Kalman Filter*. [Online]. Available: https://hal.science/hal-01122406

[39] Xsens Technologies. (2020). *MTi User Manual*. [Online]. Available: https://www.xsens.com

Ahmed M. Elsergany received the B.Sc. (summa cum laude) and M.Sc. degrees in mechanical engineering from American University of Sharjah, Sharjah, United Arab Emirates, in 2020 and 2023, respectively.

He is currently a Laboratory Instructor with the Department of Mechanical Engineering, American University of Sharjah. His research interests include modeling, nonlinear dynamics, machine health monitoring, estimation theory, and sensor fusions.

Mamoun F. Abdel-Hafez (Senior Member, IEEE) received the B.S. degree from Jordan University of Science and Technology, Irbid, Jordan, in 1997, the M.S. degree from the University of Wisconsin, Milwaukee, WI, USA, in 1999, and the Ph.D. degree from the University of California at Los Angeles (UCLA), Los Angeles, CA, USA, in 2003, all in mechanical engineering.

He was a Post-Doctoral Research Associate with the Department of Mechanical and Aerospace Engineering, UCLA, in 2003, where he was involved in a research project on fault-tolerant autonomous and multiple aircraft landing. He is currently a Professor with the Department of Mechanical Engineering, American University of Sharjah, Sharjah, United Arab Emirates. His research interests include stochastic estimation, control systems, sensor fusion, and fault detection.

Mohammad A. Jaradat received the master's and Ph.D. degrees in mechanical engineering from Texas A&M University, College Station, TX, USA, in 2002 and 2005, respectively.

He is currently with American University of Sharjah (AUS), Sharjah, United Arab Emirates, and the Mechanical Engineering Department, Jordan University of Science and Technology (JUST), Irbid, Jordan. He is also a part of the Mechatronics Graduate Program, AUS. His scientific experience has resulted in many publications, patents, projects, and awards specialized in the following research areas: robotics, artificial intelligent systems, sensor fusion, fault diagnostics, intelligent NANO-systems, intelligent control, mechatronics system design, and control systems.